Inorg. Chem. **2006**, *45*, 5742–5751

Binding Affinity of Alkynes and Alkenes to Low-Coordinate Iron

Ying Yu, Jeremy M. Smith, Christine J. Flaschenriem, and Patrick L. Holland*

Department of Chemistry, University of Rochester, Rochester, New York 14627

Received December 13, 2005

We report the synthesis, spectroscopy, and structural characterization of iron–alkyne and –alkene complexes of the type $L^{Me}Fe$(ligand) [L^{Me} = bulky β-diketiminate, ligand = HCCPh, EtCCEt, CH_2CHPh, EtCHCHEt, HCC(*p*-$C_6H_4OCH_3$), HCC(*p*-$C_6H_4CF_3$)]. The neutral ligand exchanges rapidly at room temperature, and the equilibrium constants have been measured or estimated. The binding affinity toward the low-coordinate Fe follows the trend HCCPh > EtCCEt > CH_2CHPh > EtCHCHEt ~ PPh_3 > benzene ≫ N_2. This trend is consistent with a model in which π back-bonding from the formally Fe^{I} center is the dominant interaction in determining the relative binding affinities. In nitrogenase, alkynes are reduced while alkenes are unreactive, and this work suggests that the different binding affinities to low-coordinate Fe might explain the differential activity of the enzyme toward these two substrates.

Introduction

The nitrogenase enzymes reduce not only N_2 but also a number of "alternative" substrates by multiples of $2e^-/2H^+$. The alternative substrates are small organic and inorganic compounds with multiple bonds, such as C_2H_2, CH_3NC, CO_2, COS, N_3^-, and N_2O.[1] The iron−vanadium and iron-only nitrogenases differ from iron−molybdenum nitrogenase in that they reduce acetylene to ethane as well as ethylene.[2] Simple alkenes are not nitrogenase substrates. The reasons for the selectivity of nitrogenases are not known because the mechanism of the enzymes is unclear.

The molybdenum-containing nitrogenase is the only one with detailed structural characterization, and attention has been focused on the FeMo cofactor (FeMoco; Figure 1),[3−6] the reduction site of substrates.[7,8] Crystallography has shown that this cofactor contains an octahedral Mo atom and seven Fe atoms, six of which surround an unidentified light atom

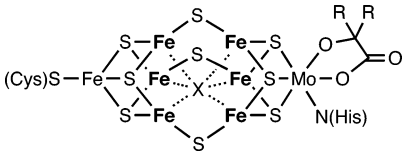

Figure 1. FeMo cofactor "FeMoco" of iron−molybdenum nitrogenase. X = C, N, or O.

X (X = C, N, or O). Electron nuclear double resonance (ENDOR) spectroscopy shows that these "belt" or "waist" Fe atoms are the site of binding for the inhibitor CO and the $2e^-/2H^+$ reduction product allyl alcohol.[1] These Fe atoms have unusually low coordination, with three bridging sulfides and a weak interaction[9,10] with the hypervalent X. Extended X-ray absorption fine structure studies suggest that the active-site clusters of molybdenum-free nitrogenases may have a similar structure.[11,12]

Because of the growing evidence for low-coordinate Fe atoms in FeMoco, synthetic low-coordinate Fe complexes

* To whom correspondence should be addressed. E-mail: holland@chem.rochester.edu.

(1) Burgess, B. K.; Lowe, D. J. *Chem. Rev.* **1996**, *96*, 2983−3011.
(2) Eady, R. R. *Chem. Rev.* **1996**, *96*, 3013−3030.
(3) Georgiadis, M. M.; Komiya, H.; Chakrabarti, P.; Woo, D.; Kornuc, J. J.; Rees, D. C. *Science* **1992**, *257*, 1653−1659.
(4) Chan, M. K.; Kim, J.; Rees, D. C. *Science* **1993**, *260*, 792−794.
(5) Peters, J. W.; Stowell, M. H. B.; Soltis, S. M.; Finnegan, M. G.; Johnson, M. K.; Rees, D. C. *Biochemistry* **1997**, *36*, 1181−1187.
(6) Mayer, S. M.; Lawson, D. M.; Gormal, C. A.; Roe, S. M.; Smith, B. E. *J. Mol. Biol.* **1999**, *292*, 871−891.
(7) Einsle, O.; Tezcan, F. A.; Andrade, S. L. A.; Schmid, B.; Yoshida, M.; Howard, J. B.; Rees, D. C. *Science* **2002**, *297*, 1696−1700.
(8) Shah, V. K.; Brill, W. J. *Proc. Natl. Acad. Sci. U.S.A.* **1977**, *74*, 3249−3253.
(9) Vrajmasu, V.; Münck, E.; Bominaar, E. L. *Inorg. Chem.* **2003**, *42*, 5974−5988.
(10) Vrajmasu, V. V.; Bominaar, E. L.; Meyer, J.; Münck, E. *Inorg. Chem.* **2002**, *41*, 6358−6371.
(11) (a) Robson, R. L.; Eady, R. R.; Richardson, T. H.; Miller, R. W.; Hawkins, M.; Postgate, J. R. *Nature* **1986**, *322*, 388−390. (b) Dilworth, M. J.; Eady, R. R.; Robson, R. L.; Miller, R. W. *Nature* **1987**, *327*, 167−168. (c) Morningstar, J. E.; Hales, B. J. *J. Am. Chem. Soc.* **1987**, *109*, 6854−6855. (d) Hales, B. J.; Case, E. E.; Morningstar, J. E.; Dzeda, M. F.; Mauterer, L. A. *Biochemistry* **1986**, *25*, 7251−7255. (e) Arber, J. M.; Dobson, B. R.; Eady, R. R.; Hasnain, S. S.; Garner, C. D.; Matsushita, T.; Nomura, M.; Smith, B. E. *Biochem. J.* **1989**, *258*, 733−737. (f) Rehder, D. *J. Inorg. Biochem.* **2000**, *80*, 133−136. (h) Eady, R. R. *Coord. Chem. Rev.* **2003**, *237*, 23−30.

10.1021/ic052136+ CCC: $33.50
Published on Web 04/21/2006

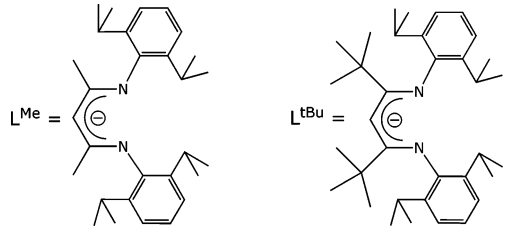

Figure 2. β-Diketiminate ligands used for the low-coordinate Fe^{I} complexes.

have been employed to gain insight into potential reaction mechanisms. Our group[13,14] and others[15] have demonstrated that three- and four-coordinate Fe bind N_2 strongly and that the N_2 complexes have unusually weak N−N bonds. The weakening is the result of back-bonding from the Fe into the π^* orbitals of N_2, which shifts the electron density onto the N_2 unit. Although the Fe atom is formally in the 1+ oxidation state, calculations suggest a substantial charge transfer from Fe to N_2 in the ground state.[14,16]

In a recent paper, we showed that one of these N_2 complexes, $L^{tBu}FeNNFeL^{tBu}$ (L^R represents the ligand shown in Figure 2), reacts with phenylacetylene to give $L^{tBu}Fe(HCCPh)$.[17] Density functional theory (DFT) calculations showed that π back-bonding again played an important role. As a low-coordinate, low-valent complex of Fe, $L^{tBu}Fe(HCCPh)$ is potentially important in understanding the nature of binding of acetylene substrates to the Fe sites in the nitrogenases.

This paper reports the synthesis, spectroscopy, and structural characterization of a wider variety of alkyne and alkene complexes of the type $L^{Me}Fe(ligand)$ [ligand = HC≡CPh (**1**), EtC≡CEt (**2**), CH_2═CHPh (**3**), EtCH═CHEt (**4**), HC≡C(*p*-$C_6H_4OCH_3$) (**5**), and HC≡C(*p*-$C_6H_4CF_3$) (**6**)].[18] To understand the binding preferences of the low-coordinate Fe center, we have measured equilibrium constants for exchange of the neutral donors. The data fit a model where π back-bonding from the Fe to the neutral ligand is the dominant interaction in determining the relative binding affinities. In addition to the implications for nitrogenase, these studies expand the known chemistry of rare high-spin Fe^{I} complexes.

Scheme 1

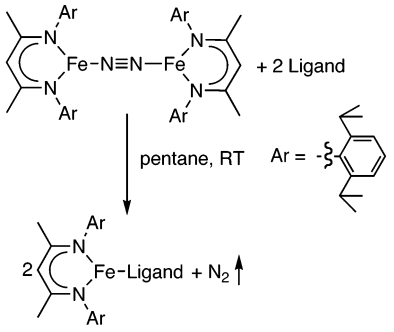

Ligand = HCCPh (**1**), EtCCEt (**2**), CH_2=CHPh (**3**), EtCH=CHEt (**4**), HCC-(p-C_6H_4-OCH_3) (**5**), HCC-(p-C_6H_4-CF_3) (**6**), PPh_3 (**7**), C_6H_6 (**8**)

We know of no previous studies describing the relative binding constants for different ligands on Fe^{I} complexes.

Results

Synthesis of Fe Complexes. As previously reported, the iron dinitrogen complex $L^{Me}FeNNFeL^{Me}$ reacts with Lewis bases to give monomeric, formally Fe^{I} products.[14] For example, the addition of 2 equiv of PPh_3 to this dinuclear N_2 complex liberates N_2 and gives 2 equiv of $L^{Me}FePPh_3$. This complex has high-spin Fe^{I} ($S = {}^3/_2$), indicated by the appearance of relatively sharp peaks in the ^{1}H NMR spectrum and by the solution magnetic moment of 3.6 μ_B.[14] On the other hand, dissolving $L^{Me}FeNNFeL^{Me}$ in benzene gives $L^{Me}Fe(C_6H_6)$, which has a broad ^{1}H NMR spectrum and an electron paramagnetic resonance signal near $g = 2$ characteristic of a low-spin configuration ($S = {}^1/_2$).[14] Each of these two complexes has been crystallographically characterized.[14]

The above substitution reaction is general for creating formally Fe^{I} complexes with alkenes and alkynes in the third coordination position, by adding 2 equiv of free ligand to a pentane solution of $L^{Me}FeNNFeL^{Me}$ (**9**; Scheme 1). At ambient temperature, the replacement of N_2 by the free ligand at the Fe center is immediate. The products are isolated by crystallization from a pentane solution, in yields of 50−80%.

The complexes are highly air- and moisture-sensitive, and in some cases, several attempts did not yield accurate C analysis on spectroscopically pure samples (^{1}H NMR spectra are given in the Supporting Information). This may be attributable to the extreme air sensitivity or to the formation of FeC. However, samples of alkene and alkyne complexes in C_6D_6 solution are thermally stable at 100 °C for 2 days.

Characterization of Alkyne Complexes. The molecular structures of **1** and **2** were determined by X-ray crystallography. ORTEP diagrams are shown in Figures 3 and 4. The important bond distances and angles are listed in Table 1.

Each alkyne has an η^2 binding mode, with the C≡C bond in a side-on interaction with the metal. The Fe distances to each C of the triple bond are comparable. This metal−ligand interaction causes considerable changes to the alkynes. The C≡C bond lengths are elongated from 1.193 Å (HCCPh) and 1.202 Å (^{t}BuC≡C^{t}Bu) in free alkyne[19,20] to 1.268(3) Å in

(12) (a) Müller, A.; Schneider, K.; Knuttel, K.; Hagen, W. R. *FEBS Lett.* **1992**, *303*, 36−40. (b) Schneider, K.; Gollan, U.; Drottboom, M.; Selsemeier-Voigt, S.; Müller, A. *Eur. J. Biochem.* **1997**, *244*, 789−800. (c) Siemann, S.; Schneider, K.; Drottboom, M.; Müller, A. *Eur. J. Biochem.* **2002**, *269*, 1650−1661. (d) Krahn, E.; Weiss, B. J. R.; Krockel, M.; Groppe, J.; Henkel, G.; Cramer, S. P.; Trautwein, A. X.; Schneider, K.; Müller, A. *J. Biol. Inorg. Chem.* **2002**, *7*, 37−45.
(13) Smith, J. M.; Lachicotte, R. J.; Pittard, K. A.; Cundari, T. R.; Lukat-Rodgers, G.; Rodgers, K. R.; Holland, P. L. *J. Am. Chem. Soc.* **2001**, *123*, 9222−9223.
(14) Smith, J. M.; Sadique, A. R.; Cundari, T. R.; Rodgers, K. R.; Lukat-Rodgers, G.; Lachicotte, R. J.; Flaschenriem, C. J.; Vela, J.; Holland, P. L. *J. Am. Chem. Soc.* **2006**, *128*, 756−769.
(15) (a) Betley, T. A.; Peters, J. C. *J. Am. Chem. Soc.* **2003**, *125*, 10782−10783. (b) Betley, T. A.; Peters, J. C. *J. Am. Chem. Soc.* **2004**, *126*, 6252−6254.
(16) Stoian, S. A.; Vela, J.; Smith, J. M.; Holland, P. L.; Bominaar, E. L.; Münck, E., submitted for publication.
(17) Stoian, S. A.; Yu, Y.; Smith, J. M.; Holland, P. L.; Bominaar, E. L.; Münck, E. *Inorg. Chem.* **2005**, *44*, 4915−4922.
(18) A related diketiminate iron(I) alkene complex $L^{Me}Fe(H_2CCPh_2)$ was reported simultaneously with this work: Bai, G.; Wei, P.; Das, A. K.; Stephan, D. W. *Dalton Trans.* **2006**, 1141.

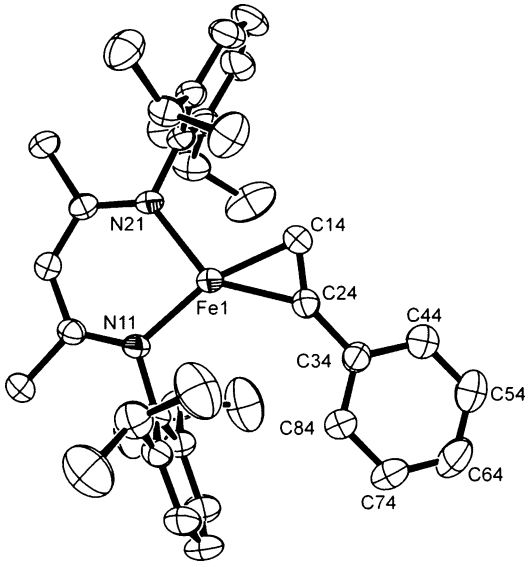

Figure 3. ORTEP drawing of the molecular structure of **1**. Thermal ellipsoids are shown at 50% probability.

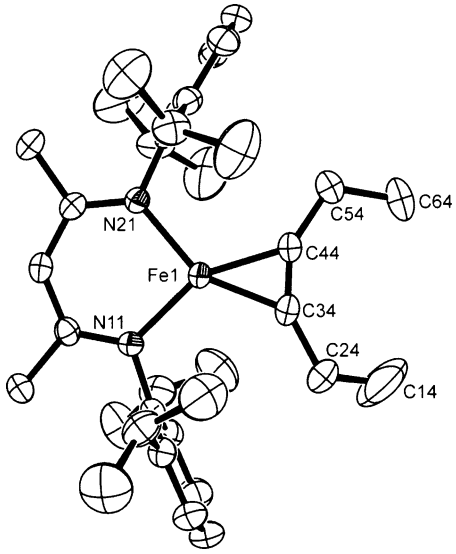

Figure 4. ORTEP drawing of the molecular structure of **2**. Thermal ellipsoids are shown at 50% probability.

Table 1. Important Bond Distances and Angles in Iron(I) Alkyne Complexes

bond/angle	HCCPh	EtCCEt
Fe−N (Å)	1.973(1), 1.990(1)	1.986(2), 1.983(2)
Fe−C (Å)	1.917(2), 1.958(2)	1.932(3), 1.944(3)
C≡C (Å)	1.268(3)	1.263(4)
C≡C−C (deg)	143.8(2)	148.9(3), 148.5(3)
N−Fe−N (deg)	93.67(6)	93.75(8)

1 and 1.263(4) Å in **2**. The C≡C−C angles are bent significantly from the ideal 180° for sp-hybridized C to 143.8(2)° for HCCPh and 148.7(5)° for EtCCEt. The C≡C bonds are nearly coplanar with the N−Fe−N plane. This roughly square-planar geometry gives the idealized point group C_{2v} for **2** and C_s in **1**.

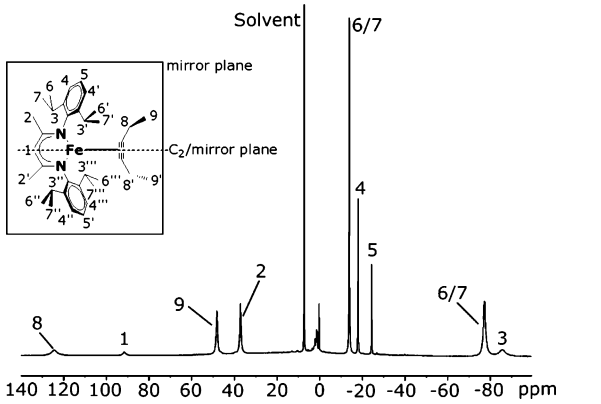

Figure 5. ^{1}H NMR spectrum of **2** in benzene-d_6 at 298 K. Inset: assignments of equivalent protons.

The solution magnetic moment (measured through the method of Evans[21]) is 4.7(7) for **1** and 4.4(8) for **2**, consistent with high-spin Fe^{I} ($S = {}^3/_2$). Consistent with other diketiminate complexes of Co^{II} and Fe^{I} with a d^7 configuration,[17,22] the alkyne complexes show distinct ^{1}H NMR resonances in a wide range from +130 to −100 ppm. The ^{1}H NMR spectrum of **2** in Figure 5 exemplifies the assignment of the spectra. Proton peaks belonging to the β-diketiminate ligand are assigned based on the integrations. As in previous complexes reported by our group,[22] the diketiminate ligand displays seven peaks, which are labeled in the inset of Figure 5. The eight isopropyl methyl groups fall into two categories: four point toward the Fe center while four point away. The chemical shifts of the diketiminate proton peaks are similar to those in L^{tBu}Fe(HCCPh).[17] The proton signals of the bound alkyne have an upfield paramagnetic shift. The spectrum of **2** is thus consistent with that expected for averaged C_{2v} symmetry, showing that there is free rotation of the C−C bonds of the alkyne ligand.

The room-temperature ^{1}H NMR spectrum of L^{Me}Fe(PhCCH) is also consistent with that expected for C_{2v} symmetry, despite the C_s symmetry of the molecule. We hypothesized that there is rapid spinning of the alkyne around the axis connecting the Fe to the C≡C centroid on the NMR time scale. This was tested by lowering the temperature of a toluene-d_8 solution of **1**. Decoalescence of the isopropyl groups was observed, with a coalescence temperature of about −55 °C (see the Supporting Information for spectra and details), yielding a barrier for alkyne rotation of 33 kJ mol^{-1} (8 kcal mol^{-1}). The barrier for hindered rotation of the alkyne is less in this complex than in the Cu^{I} analogue.[23]

Each alkyne complex shows a weak-to-medium C≡C stretching band that shifts from around 2100 cm^{-1} in the free ligand to 1700−1800 cm^{-1} upon coordination (Table 2). To examine the effect of differential electronic effects

(19) (a) Harmony, M. D.; Laurie, V. W.; Kuczkowski, R. L.; Schwendeman, R. H.; Ramsay, D. A.; Lovas, F. J.; Lafferty, W. J.; Maki, A. G. *J. Phys. Chem. Ref. Data* **1979**, *8*, 619−721. (b) Lide, D. R., Jr. *Tetrahedron* **1962**, *17*, 125−134. (c) Weiss, H.-C.; Blaser, D.; Boese, R.; Doughan, B. M.; Haley, M. M. *Chem. Commun.* **1997**, 1703−1704.

(20) The bond distance of the C−C triple bond in EtCCEt is not available, so ^{t}BuCC^{t}Bu is used. Boese, R.; Bläser, D.; Latz, R.; Bäumen, A. *Acta Crystallogr.* **1999**, *55C*, IUC9900016.

(21) Evans, D. F. *J. Chem. Soc.* **1959**, 2003−2005.

(22) Holland, P. L.; Cundari, T. R.; Perez, L. L.; Eckert, N. A.; Lachicotte, R. J. *J. Am. Chem. Soc.* **2002**, *124*, 14416−14424.

(23) Badiei, Y. M.; Warren, T. H. *J. Organomet. Chem.* **2005**, *690*, 5989−6000.

Table 2. C≡C Stretching Frequencies in Alkyne Complexes

complex	ligand	ν (cm^{-1})	ν_{free} (cm^{-1})	$\Delta\nu$ (cm^{-1})
2	EtC≡CEt	1802	2120	318
1	HC≡CPh	1717	2110	393
5	HC≡C(*p*-$C_6H_4OCH_3$)	1717	2106	389
6	HC≡C(*p*-$C_6H_4CF_3$)	1720	2118	398

Table 3. Electronic Absorption Spectra of Alkyne Complexes

complex	alkyne ligand	λ_{max}/nm (ϵ/mM^{-1} cm^{-1})
1	HC≡CPh	328 (15.7), 395 (6.8), 524 (0.6), 738 (0.2)
2	EtC≡CEt	329 (12.3), 395 (7.2), 512 (0.6)
5	HC≡C(*p*-$C_6H_4OCH_3$)	328 (15.4), 395 (6.2), 520 (0.6), 715 (0.2)
6	HC≡C(*p*-$C_6H_4CF_3$)	328 (14.7), 395 (5.9), 527 (0.6), 734 (0.2)

of the acetylene ligand, phenylacetylenes with different para substituents were also examined. Table 2 demonstrates that the substituent affects the amount by which the C≡C frequency decreases upon coordination, with more electron-withdrawing substituents giving a larger coordination-induced weakening.

UV−vis spectrophotometry is used below to distinguish different Fe species in solution. The absorption maxima (λ_{max}) and extinction coefficients are summarized in Table 3. The very intense band around 330 nm is seen in many different diketiminate complexes,[24] and we assign it as a diketiminate $\pi \rightarrow \pi^*$ transfer. The band near 520 nm shifts to lower energy with electron-withdrawing groups on the acetylene, consistent with assignment as an Fe → acetylene metal-to-ligand charge-transfer transition.

Characterization of Alkene Complexes. The molecular structures of the alkene−iron complexes were determined by X-ray diffraction, and the ORTEP diagrams of **3** and **4** are shown in Figures 6 and 7.

The structure of **4** contains a disordered CH_3CH_2CH═$CHCH_2CH_3$ group. C34 and C44 of the hexene are disordered in a 1:2 ratio for parts A and B, respectively (parts A and B refer to the two conformations). All of the C═C double-bond lengths are larger than expected for a sp^2−sp^2 double bond but are equivalent between parts A and B.

The alkenes bind through an η^2 interaction of the C═C double bond to the Fe center, analogous to the alkyne complexes described above. The alkene C═C bond is neither in the diketiminate plane (analogous to the alkyne complexes) nor perpendicular to it. The angle between the N−Fe−N plane and the Fe−C−C plane in **3** is 19.3(6)°, with the phenyl ring pointing out of the N−Fe−N plane; the analogous angle in **4** is 42.5(3)°, with the ethyl substituents near the N−Fe−N plane. Similarly to the alkyne complexes, the double bond in the alkene ligands is weakened. The C═C bond distance (Table 4) is elongated from 1.34 Å in a typical alkene[25] to 1.401(8) and 1.420(4) Å for EtCH═CHEt and 1.396(5) Å for CH_2═CHPh. A similar C═C elongation has been observed in L^{Me}Fe(Ph_2C═CH_2), with C−C = 1.411 Å.[18] Also, the C═C−C angles are slightly larger than the expected 120° value for sp^2-hybridized C [125.1(3)°, 124.4(3)°, 125.5(5)°, and 130.1(6)° for **4** and 124.5(4)° for **3**].

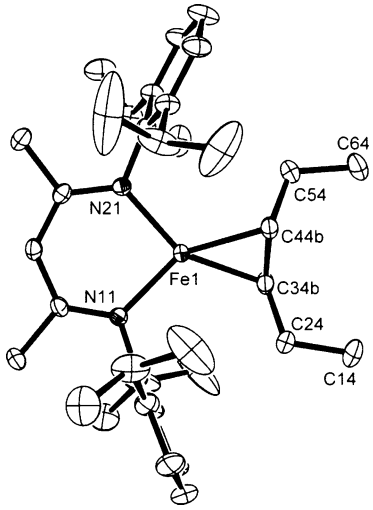

Figure 6. ORTEP drawing of the molecular structure of **4**. Thermal ellipsoids are shown at 50% probability. The EtCH═CHEt groups are disordered over two conformations in a 2:1 ratio, and the major conformer is shown.

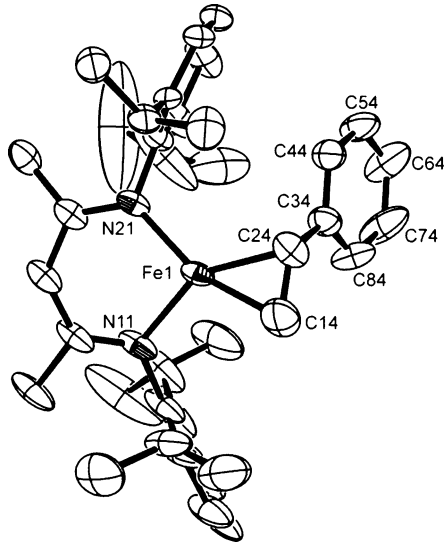

Figure 7. ORTEP drawing of the molecular structure of **3**. Thermal ellipsoids are shown at 50% probability.

The alkene complexes have ^{1}H NMR spectra that are paramagnetically shifted, like those of the alkyne complexes. However, the lower symmetry makes the ^{1}H NMR spectra of alkene complexes more complicated. For example, the ^{1}H NMR spectrum of the complex **3** is shown in Figure 8. In complex **3**, the styrene ligand binds to Fe through the C═C π orbital. In this binding mode, the styrene phenyl ring extends out of the N−Fe−N plane, breaking both mirror planes. As a result, the pairs of protons that were equivalent

(24) (a) Spencer, D. J. E.; Reynolds, A. M.; Holland, P. L.; Jazdzewski, B. A.; Duboc-Toia, C.; Le Pape, L.; Yokota, S.; Tachi, Y.; Itoh, S.; Tolman, W. B. *Inorg. Chem.* **2002**, *41*, 6307−6321. (b) Randall, D. W.; George, S. D.; Holland, P. L.; Hedman, B.; Hodgson, K. O.; Tolman, W. B.; Solomon, E. I. *J. Am. Chem. Soc.* **2000**, *122*, 11632−11648. (c) Panda, A.; Stender, M.; Wright, R. J.; Olmstead, M. M.; Klavins, P.; Power, P. P. *Inorg. Chem.* **2002**, *41*, 3909−3916. (d) Vela, J.; Smith, J. M.; Yu, Y.; Ketterer, N. A.; Flaschenriem, C. J.; Lachicotte, R. J.; Holland, P. L. *J. Am. Chem. Soc.* **2005**, *127*, 7857−7870.

(25) Cochran, J. C.; Hagen, K.; Paulen, G.; Shen, Q.; Tom, S.; Traetteberg, M.; Wells, C. *J. Mol. Struct.* **1997**, *413*−*414*, 313−326.

Table 4. Bond Distances and Angles in Alkene−Iron(I) Complexes

bond/angle	CH_2═CHPh	EtCH═CHEt	CH_2═CPh_2[18]
Fe−N (Å)	1.968(2), 1.986(2)	1.989(1), 1.992(1)	1.967(2), 2.001(2)
Fe−C (Å)	2.013(4), 2.027(3)	2.036(5), 2.039(4) (A) 2.047(3), 2.053(2) (B)	1.995(2), 2.089(2)
C═C (Å)	1.396(5)	1.401(8) (A) 1.420(4) (B)	1.411(3)
N−Fe−N (deg)	95.81(10)	93.84(5)	95.08(8)
C═C−C (deg)	124.5(4)	130.1(6), 125.5(5) (A) 125.1(3), 124.4(3) (B)	

Table 5. UV−Vis Absorption Data

complex	alkene ligand	λ_{max}/nm (ϵ/mM^{-1} cm^{-1})
3	CH_2═CHPh	319 (18.8), 374 (11.7)
4	EtCH═CHEt	315 (18.4), 367 (10.4), 471 (1.9)

in the alkyne complexes (such as 3 and 7 in the inset of Figure 8) are not equivalent in **3**. However, the NMR spectrum shows only two types of isopropyl groups and one type of backbone methyl group, suggesting rapid rotation of the styrene ligand that gives averaged C_2 symmetry.[26] Variable-temperature ^{1}H NMR spectra over a range from +70 to −70 °C showed no changes in the number of peaks, indicating that the alkene remains coordinated but spins rapidly on the NMR time scale.

The bands in the IR spectrum corresponding to the C═C double bonds in alkene ligands were not assigned because the C═C stretching region of the spectrum is obscured by vibrations of the β-diketiminate supporting ligand. UV−vis spectral data for the alkene complexes are listed in Table 5. The band at 315−320 nm is assigned as a $\pi \rightarrow \pi^*$ transition of the β-diketiminate supporting ligand, as for the alkyne complexes above.

The other formally Fe^I complexes used here, in which the non-diketiminate ligand is PPh_3, C_6H_6, and N_2, have been described previously.[14]

Ligand Binding Affinities. The differences between the visible spectra of the different complexes are sufficient to make UV−vis spectrophotometry a convenient technique for determining the relative concentrations of different Fe complexes in solution. When a donor ligand is added to an Fe complex of another donor ligand, equilibrium is established rapidly in solution, and the equilibrium constant can be interpreted as shown in eq 1.

$$L^{Me}Fe(\text{ligand A}) + \text{ligand B} \overset{K_{eq}}{\rightleftharpoons} L^{Me}Fe(\text{ligand B}) + \text{ligand A}$$

$$K_{eq} = \frac{[L^{Me}Fe(\text{ligand B})][\text{ligand A}]}{[L^{Me}Fe(\text{ligand A})][\text{ligand B}]} \quad (1)$$

In a typical experiment, one Fe complex $L^{Me}Fe$(ligand A) is dissolved in pure solvent, and excess amounts (at least 50 times the Fe concentration) of both ligands A and B are added. Assuming that the concentrations of the ligands remain unchanged and that the ligands are transparent in the visible region, the visible spectra give the ratio of concentrations of the two Fe complexes, leading to the equilibrium constants (eq 1). The equilibrium constants determined in this way are shown in Table 6. Unfortunately, equilibrium constants could not be measured in cases where neat ligand B did not give a detectable amount of $L^{Me}Fe$(ligand B). In these cases, we use a conservative estimated UV−vis detection limit of 5% to derive lower limits for the equilibrium constants. More detailed measurement data are in the Supporting Information (Table S1).

Table 6. Equilibrium Constants for Ligand Exchange Reactions

ligand A	ligand B	K_{eq}
EtC≡CEt	HC≡CPh	$(1.2 \pm 0.2) \times 10^2$
H_2C═CHPh	EtC≡CEt	$\geq(1.7 \pm 0.3) \times 10^5$
EtCH═CHEt	H_2C═CHPh	$(1.2 \pm 0.3) \times 10^2$
PPh_3	EtCH═CHEt	2.0 ± 0.7
C_6H_6	PPh_3	65 ± 20
N_2	C_6H_6	$\geq(3.7 \pm 0.2) \times 10^2$ [a]
HC≡CPh	HC≡C(*p*-$C_6H_4CF_3$)	6.0 ± 0.7
HC≡C(*p*-$C_6H_4OCH_3$)	HC≡CPh	1.1 ± 0.4

[a] The N_2 concentration is estimated using the solubility of N_2 in pentane at STP.[27,28]

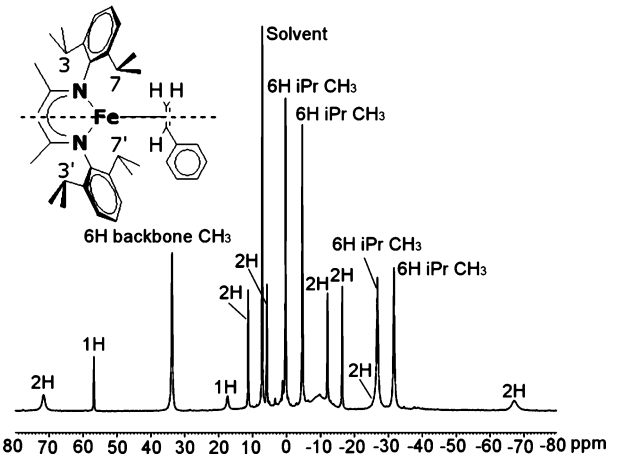

Figure 8. ^{1}H NMR spectrum of **3** in benzene-d_6 at 298 K. Inset: assignments of equivalent protons.

N_2 was completely displaced by each of the ligands, giving a lower limit of $K_{eq} > 3.7 \times 10^2$. The alkynes bind to Fe^I much more strongly than the alkenes, and even adding neat alkene to an iron(I) alkyne complexes did not give a detectible amount of alkene complex. In both the alkenes and alkynes, the alkyl-substituted compound (*trans*-3-hexene or 3-hexyne) binds more weakly than the aryl-substituted compound (styrene or phenylacetylene). Triphenylphosphine and 3-hexene bind equally strongly, but each of these binds more strongly than benzene. These data are depicted on an energy scale in Figure 9.

(26) Apparent NMR equivalence in diketiminate iron complexes with no symmetry element: Vela, J.; Vaddadi, S.; Cundari, T. R.; Smith, J. M.; Gregory, E. A.; Lachicotte, R. J.; Flaschenriem, C. J.; Holland, P. L. *Organometallics* **2004**, *23*, 5226−5239.

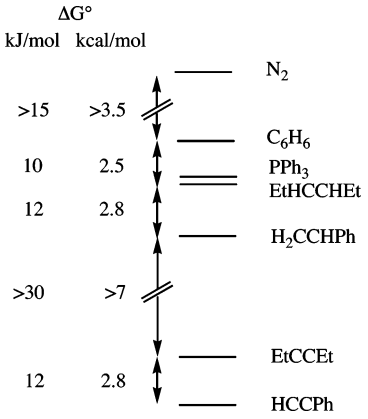

Figure 9. Relative binding energies for different ligands, with the most strongly bound ligands at the bottom. In some cases, only a lower limit on the energy difference could be determined. The precision of the values is better than 1 kJ mol^{-1} (0.2 kcal mol^{-1}).

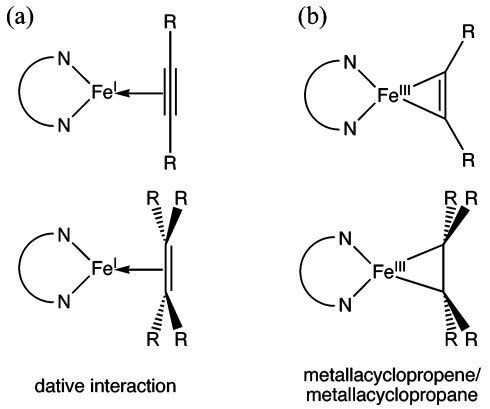

Figure 10. Limiting resonance structures for metal−alkyne and metal−alkene complexes. Though these descriptions are exaggerated, they help to rationalize the properties of the iron−alkene and iron−alkyne complexes described here.

Discussion

Synthesis and Isolation of Stable Mononuclear Fe Complexes with a Formal Oxidation State of 1+. The number of mononuclear Fe^{I} complexes is much fewer than Fe^{II} and Fe^{III} species. Most work on Fe^{I} has focused on gas-phase Fe^{+} ions, which are capable of C−C and C−H bond activation.[29] However, these are not isolable, leaving the further characterization of Fe^{I} as a challenge for synthetic chemists. Cyclopentadienyl- and arene-containing organometallic complexes account for a large fraction of known Fe^{I} complexes.[30] Strong back-bonding ligands stabilize Fe^{I} in $[Fe(CO)_x(PR)_y]^{+}$ [31] and nitrosyl complexes.[32] Several examples of formally Fe^{I} centers supported by porphyrin have been reported, although there is controversy over whether the best description of the complexes is Fe^{II}(porph$^{\bullet-}$) or Fe^{I}(porph).[33] This ambiguity in the oxidation states is also evident in complexes of some S-based ligands.[34] Complexes of other N_4 macrocyclic ligands are typically formulated as Fe^{I}.[35] There is a single example of an iron(I) hydride complex.[36] A more recent approach to isolating formally Fe^{I} compounds uses sterically hindered ligands. Examples of this type of complex include PhTp^{tBu}Fe(CO), [PhBP$_3$]Fe(PPh$_3$),[15] and (^{i}PrPDI)FeX (X = Cl, Me).[37] However, the fundamental coordination chemistry of low-coordinate Fe^{I} complexes is still under development.

In this work, we show that displacement of N_2 in L^{Me}-FeNNFeL^{Me} gives a variety of complexes of the type L^{Me}-Fe(ligand). This substitution reaction provides a general route to low-coordinate, formally Fe^{I} complexes with various Lewis bases as the second binding ligand. We previously described the addition of PPh$_3$, CO, and benzene to L^{Me}-FeNNFeL^{Me} to give L^{Me}FePPh$_3$, L^{Me}Fe(CO)$_3$, and L^{Me}-(benzene).[14] Here, we focus on alkene and alkyne complexes and use measurements of K_{eq} to compare the binding of these ligands to the phosphine and arene ligands.

Evaluation of C−C Bonding. Alkene and alkyne complexes can be described in terms of the two limiting resonance structures shown in Figure 10.[38] (a) In one extreme, the metal has a primarily electrostatic interaction with the ligand (best described through the dative interaction at the left of Figure 10). For example, in alkyne complexes of Ag, the C−C distance and C−C stretching frequency are similar to those in the free ligand.[39] Because the primary metal−ligand interaction is donation of ligand electrons to

(27) Battino, R.; Rettich, T. R.; Tominaga, T. *J. Phys. Chem. Ref. Data* **1984**, *13*, 563−600.
(28) Makranczy, J.; Megyery-Balog, M. K.; Rusz, L.; Patyi, L. *Hung. J. Ind. Chem.* **1976**, *4*, 269−280.
(29) (a) Wesendrup, R.; Schalley, C. A.; Schroeder, D.; Schwarz, H. *Organometallics* **1996**, *15*, 1435−1440. (b) Schalley, C. A.; Wesendrup, R.; Schroeder, D.; Schroeter, K.; Schwarz, H. *J. Am. Chem. Soc.* **1995**, *117*, 12235−12242. (c) Schroeder, D.; Schwarz, H. *J. Organomet. Chem.* **1995**, *504*, 123−135. (d) Schalley, C. A.; Schroeder, D.; Schwarz, H. *J. Am. Chem. Soc.* **1994**, *116*, 11089−11097. (e) Peake, D. A.; Gross, M. L. *Organometallics* **1986**, *5*, 1236−1243.
(30) (a) Hamon, P.; Toupet, L.; Hamon, J.-R.; Lapinte, C. *Organometallics* **1996**, *15*, 10−12. (b) Hamon, P.; Toupet, L.; Hamon, J.-R.; Lapinte, C. *Organometallics* **1996**, *15*, 10−12. (c) Lapinte, C.; Catheline, D.; Astruc, D. *Organometallics* **1984**, *3*, 817−819. (d) Astruc, D.; Mandon, D.; Madonik, A.; Michaud, P.; Ardoin, N.; Varret, F. *Organometallics* **1990**, *9*, 2155−2164.
(31) (a) Therien, M. J.; Ni, C. L.; Anson, F. C.; Osteryoung, J. G.; Trogler, W. C. *J. Am. Chem. Soc.* **1986**, *108*, 4037−4042. (b) MacNeil, J. H.; Chiverton, A. C.; Fortier, S.; Baird, M. C.; Hynes, R. C.; Williams, A. J.; Preston, K. F.; Ziegler, T. *J. Am. Chem. Soc.* **1991**, *113*, 9834−9842. (c) Kandler, H.; Gauss, C.; Bidell, W.; Rosenberger, S.; Buergi, T.; Eremenko, I. L.; Veghini, D.; Orama, O.; Burger, P.; Berke, H. *Chem.—Eur. J.* **1995**, *1*, 541−548.
(32) (a) Stokes, S. L.; Davis, W. M.; Odom, A. L.; Cummins, C. C. *Organometallics* **1996**, *15*, 4521−4530. (b) Manhas, B. S.; Kalia, S. B. *Polyhedron* **1996**, *15*, 2949−2952.
(33) (a) Pawlicki, M.-L.; Latos-Grazynski, L. *Inorg. Chem.* **2002**, *41*, 5866−5873. (b) Mashiko, T.; Reed, C. A.; Haller, K. J.; Scheidt, W. R. *Inorg. Chem.* **1984**, *23*, 3192−3196. (c) Rodgers, K. R.; Reed, R. A.; Su, Y. O.; Spiro, T. G. *Inorg. Chem.* **1992**, *31*, 2688−2700.
(34) (a) Williams, R.; Billig, E.; Waters, J. H.; Gray, H. B. *J. Am. Chem. Soc.* **1966**, *88*, 43−50. (b) Gray, H. B.; Billig, E. *J. Am. Chem. Soc.* **1963**, *85*, 2019−2020.
(35) (a) Klose, A.; Hesschenbrouck, J.; Solari, E.; Latronico, M.; Floriani, C.; Re, N.; Chiesi-Villa, A.; Rizzoli, C. *J. Organomet. Chem.* **1999**, *591*, 45−62. (b) Rakowski, M. C.; Busch, D. H. *J. Am. Chem. Soc.* **1975**, *97*, 2570−2571.
(36) Gargano, M.; Giannoccaro, P.; Rossi, M.; Vasapollo, G.; Sacco, A. *J. Chem. Soc., Dalton Trans.* **1975**, 9−12.
(37) Bouwkamp, M. W.; Bart, S. C.; Hawrelak, E. J.; Trovitch, R. J.; Lobkovsky, E.; Chirik, P. J. *Chem. Commun.* **2005**, 3406−3408.
(38) (a) Hartley, F. R. *Angew. Chem., Int. Ed. Engl.* **1972**, *11*, 596−606. (b) Boston, J. L.; Grim, S. O.; Wilkinson, G. *J. Chem. Soc.* **1963**, 3468−3470. (c) Frenking, G.; Fröhlich, N. *Chem. Rev.* **2000**, *100*, 717−774.
(39) (a) Dias, H. V. R.; Wang, Z.; Jin, W. *Inorg. Chem.* **1997**, *36*, 6205−6215. (b) Chi, K.-M.; Lin, C.-T.; Peng, S.-M.; Lee, G.-H. *Organometallics* **1996**, *15*, 2660−2663.

the metal, *electron-donating* substituents are expected to increase the binding constant.[40,41] (b) At the other extreme, there is a covalent interaction between the metal and the bound C atoms (best described through the metallacyclopropene or metallacyclopropane structures in Figure 10). Because two electrons are formally transferred from the metal to the ligand, *electron-withdrawing* groups on the ligand should increase the binding constant and weaken the C−C bond relative to the free ligand. The decreased C−C bond order and the rehybridization of the C atoms in alkyne complexes are reflected especially in elongation of the C−C bond, a decrease of the C≡C stretching frequency, and bending of the C≡C−C angle (although the latter effect could also result from steric effects). In alkene complexes, analogous structural distortions are expected, with pyramidalization of the bound C atoms.

The alkene and alkyne complexes described here clearly have a substantial contribution from the second resonance structure. Both C≡C and C=C bonds are elongated by about 0.06 Å relative to the free alkyne−alkene. In alkyne complexes, the C≡C−C angle is bent to 143.8(2)−148.9(3)°. In addition, the C−C stretching frequencies decrease by about 390 cm^{-1} in the formally Fe^{I} complexes, from about 2100 to 1700−1800 cm^{-1} (Table 2). The alkynes that bear electron-withdrawing groups have larger decreases in the C−C stretching frequency ($\Delta\nu$) upon coordination. While the changes are only about 1−2% of $\Delta\nu$, the monotonic changes are greater than the precision of IR measurements. The larger C≡C bond weakening with electron-withdrawing groups is consistent with a model where bonding involves substantial donation of metal electrons into the ligand. On the basis of the combined evidence, we conclude that back-bonding is the dominant metal−ligand interaction in these low-coordinate Fe complexes.

These experimental results are also consistent with DFT calculations on L^{tBu}Fe(HCCPh) that showed a buildup of 0.8 electrons of negative charge on HCCPh.[17] *Therefore, while "Fe^{I}" is an accurate description of the formal oxidation state, there is actually substantial charge transfer from Fe to acetylene.*

Surprisingly, the back-bonding in these formally Fe^{I} complexes is more than that in most literature Fe^{0} complexes. VISTA analysis of formally iron(0) alkyne complexes in the Cambridge Structural Database[42] gave an average C≡C bond distance of 1.24(1) Å and an average C≡C−C angle of 152(4)°. The C≡C distances of the formally iron(I) alkyne complexes described here are about 0.02 Å longer than those of the average literature iron(0) alkyne complex, and the C≡C−C angles are several degrees smaller. Given the similarity in electronic structure to related N_2 complexes[13] and the theoretical analysis of L^{tBu}Fe(HCCPh),[17] it is reasonable to conclude that the low-coordinate geometry of the diketiminate complexes leads to anomalous weakening beyond that expected from the formal oxidation state. In support of this idea, the recently reported low-coordinate iron(0) alkyne complex (^{i}PrPDI)Fe(PhCCPh) has a C−C distance of 1.283(6) Å, similar to those in the complexes described here.[43]

Table 7. Ligand Binding Trends

HCCPh > EtCCEt > CH_2=CHPh > EtCH=CHEt ~ PPh_3 > C_6H_6 ≫ N_2						
K_{eq}	120	$\geq 1.7 \times 10^5$	120	2	65	≥370
ΔG/kJ mol^{-1}	12	≥30	12	2	10	≥15

HCC(p-$C_6H_4CF_3$) > HCCPh ~ HCC(p-$C_6H_4OCH_3$)		
K_{eq}	6.0	1.1
ΔG/kJ mol^{-1}	4	1

Competitive Binding of Ligands to Low-Coordinate Fe. One of the fundamental properties of a metal center is its preference for different ligands. Only a few reports in the literature systematically study the binding preferences of low-coordinate transition-metal complexes.[40,44−46]

Here we give relative ligand binding constants for low-coordinate, formally Fe^{I} complexes, determined using UV−vis spectroscopy. Because the characteristic color changes upon ligand addition occur over a few seconds at room temperature, the UV−vis measurements reflect equilibrium ratios. Crystallography shows that all of the complexes (except the N_2 complex) are 1:1 metal−ligand complexes, and therefore the reaction entropy should be nearly zero. Therefore, the binding affinities can be interpreted in enthalpic terms. This is the case for all ligands except N_2, which forms a 2:1 complex and involves a gas. The data are summarized in Table 7.

To evaluate electronic effects, we measured the equilibrium constants of the substitutions of substituted phenylacetylenes. The substitution at the para position of the phenyl ring is expected to have a minimal steric effect on the complex. This is supported by the crystal structure of **1**, which shows that the para hydrogen is more than 5 Å from every atom of the β-diketiminate ligand. The electron-donating methoxy group disfavors binding of phenylacetylene. In most complexes of neutral donor ligands, electron-donating groups magnify metal−ligand bonding.[40,41] The preference for electron-withdrawing groups is more characteristic of ligands that are "anionic" (using ionic electron-counting conventions)[47] and indicates that back-bonding is the dominant interaction in determining the metal−ligand

(40) (a) Kurosawa, H.; Asada, N. *Organometallics* **1983**, *2*, 251−257. (b) Kurosawa, H.; Urabe, A.; Emoto, M. *J. Chem. Soc., Dalton Trans.* **1986**, 801−893. (c) Kurosawa, H.; Miki, K.; Kasai, N.; Ikeda, I. *Organometallics* **1991**, *10*, 1607−1613. (d) Ohkita, K.; Kurosawa, H.; Hirao, T.; Ikeda, I. *J. Organomet. Chem.* **1994**, *470*, 189−190.

(41) This trend has been observed in the relative binding enthalpy for phosphines. For examples, see: (a) Rahman, M. M.; Liu, H. Y.; Prock, A.; Giering, W. P. *Organometallics* **1987**, *6*, 650−658. (b) Li, C.; Nolan, S. P. *Organometallics* **1995**, *14*, 1327−1332. However, exceptions are known: (c) Landis, C. R.; Feldgus, S.; Uddin, J.; Wozniak, C. E.; Moloy, K. G. *Organometallics* **2000**, *19*, 4878−4886.

(42) CSD version 1.7 (updated May 2005) and Vista version 2.1 were used. Allen, F. H. *Acta Crystallogr.* **2002**, *B58*, 380−388.

(43) Bart, S. C.; Lobkovsky, E.; Chirik, P. J. *J. Am. Chem. Soc.* **2004**, *126*, 13794−13807.

(44) (a) Wang, K.; Goldman, A. S.; Li, C.; Nolan, S. P. *Organometallics* **1995**, *14*, 4010−4013. (b) Wang, K.; Rosini, G. P.; Nolan, S. P.; Goldman, A. S. *J. Am. Chem. Soc.* **1995**, *117*, 5082−5088. (c) Rosini, G. P.; Liu, F.; Krogh-Jespersen, K.; Goldman, A. S.; Li, C.; Nolan, S. P. *J. Am. Chem. Soc.* **1998**, *120*, 9256−9266.

(45) Popp, B. V.; Thorman, J. L.; Morales, C. M.; Landis, C. R.; Stahl, S. S. *J. Am. Chem. Soc.* **2004**, *126*, 14832−14842.

(46) Stroemberg, S.; Svensson, M.; Zetterberg, K. *Organometallics* **1997**, *16*, 3165−3168.

(47) Holland, P. L.; Andersen, R. A.; Bergman, R. G.; Huang, J.; Nolan, S. P. *J. Am. Chem. Soc.* **1997**, *119*, 12800−12814 and references cited therein.

binding energy in these acetylene complexes.[48,49] This conclusion is concordant with the greater C−C bond weakening in the complexes with more electron-withdrawing groups, observed by IR spectroscopy (see above). In the following discussion, we show that the other data can also be rationalized by invoking the primacy of back-bonding in metal−ligand affinity.

Our experimental data indicate that alkynes are the best ligands toward the formally Fe^{I} center, binding much more strongly ($K_{eq} > 1.7 \times 10^5$) than alkenes. A similar binding trend has been reported for gas-phase ligation of Fe^{I}, where the relative affinity was alkynes > alkenes > alkanes.[50] The reasons why alkynes bind more strongly to transition metals than alkenes are not clear. Using the back-bonding model presented above, one might guess that alkynes have more tendency to accept charge than alkenes.[51] We suggest tentatively that the availability of more π interactions in the diketiminate iron−alkyne complexes enables greater orbital mixing and stabilization of the complex. We hope that the results presented here motivate further spectroscopic and theoretical work in this area.

Surprisingly, PPh_3 is a weaker ligand than alkynes and alkenes for the low-coordinate Fe complexes described here. This observation is different from most organometallic complexes, where P has high affinity for late transition metals (soft acids). However, triarylphosphines are not strong π acceptors,[52] so this observation fits a model where π back-bonding dominates the stability of the complex. The poor binding affinity may also be due to steric effects: in the crystal structure, the phosphine has one phenyl group in proximity to two isopropyl groups of the diketiminate. A variable-temperature NMR study of $L^{Me}FePPh_3$ indicates that rotation of the Fe−P bond is restricted on the NMR time scale at −25 °C.[14]

Benzene binds to the diketiminate iron complexes fairly weakly and, of the ligands studied here, is able to displace only N_2. This trend is more general: in the styrene and phenylacetylene complexes, styrene binds to Fe through the alkene−alkyne bond instead of the phenyl ring. In the literature, different preferences have been observed. For example, an Os complex prefers binding to the triple bond of phenylacetylene,[53] but an Fe complex prefers arene binding.[54]

Potential intermediate for nitrogenase $L^{Me}Fe(CH_2{=}CHPh)$

Figure 11. Comparison of the structure assigned to a spectroscopically observed intermediate in nitrogenase (left)[58,59] and the alkene−metal unit found in $L^{Me}Fe$(styrene) (right).

N_2 is the weakest binding substrate in this work. However, the enthalpic reasons for this result are difficult to interpret because the release of N_2 gas entropically drives the substitution reaction. Therefore, a quantitative comparison of N_2 to the other ligands is difficult at this time.

Possible Implications for Nitrogenase. The mechanism of nitrogen fixation by nitrogenase is still obscure after decades of intense research. ENDOR studies on nitrogenase enzymes with mutation at α-Val70 have given detectable intermediates in which substrates are bound toFeMoco, including protons,[55] hydrazine,[56] and alkynes.[57] In each case, binding is proposed to take place at one of the central Fe atoms of FeMoco. The crystal structure of **3** shares common features with an FeMoco complex that has been freeze-trapped during propargyl alcohol reduction by nitrogenase (Figure 11).[58,59] Studies of the pH dependence of different mutants, geometric considerations, and theoretical calculations led to a model in which the product (allyl alcohol) is bound to a single Fe atom of the cofactor. The authors formulate this as an allyl alcohol complex, which exists as a metallacylopropane, the result of substrate reduction by two electrons. This interpretation is in concert with our results on synthetic low-coordinate Fe complexes, in which there is substantial charge transfer from the metal to the ligand. ENDOR studies of the alkene and alkyne complexes reported here are underway and are expected to provide further comparisons between the synthetic and biological chemistry of low-coordinate Fe complexes.

Small alkynes are common substrates for nitrogenase, but alkenes are very poor substrates.[1] When acetylene is reduced by nitrogenase, ethene is observed as a major product, with less than 1% ethane.[60] The underlying reason for the differential reactivity toward alkenes and alkynes is unknown. The relative binding affinities of our model complexes provide an initial clue because alkynes bind more than 150 000 times stronger to the low-coordinate iron center.[61] Although the coordination geometry and oxidation state of

(48) Theoretical calculations show that the energy of deforming the ligand is also important. Cedeño, D. L.; Weitz, E. *J. Am. Chem. Soc.* **2001**, *123*, 12857−12865.
(49) This trend has also been seen for pyridine complexes, which can act as π acceptors: *Pol. J. Chem.* **1987**, *61*, 735−745.
(50) Baranov, V.; Becker, H.; Bohme, D. K. *J. Phys. Chem. A* **1997**, *101*, 5137−5147.
(51) Both alkenes and alkynes have negative electron affinities (the anions are unbound). Experimental electron attachment energies indicate that alkynes have more negative electron affinities, but high-level computations indicate that alkenes have more negative electron affinities. This makes it difficult to gauge the inherent ability of these groups to accept electron density. (a) Jordan, K. D.; Burrow, P. D. *Acc. Chem. Res.* **1978**, *11*, 341−348. (b) Zhan, C.-G.; Nichols, J. A.; Dixon, D. A. *J. Phys. Chem. A* **2003**, *107*, 4184−4195.
(52) Orpen, A. G.; Connelly, N. G. *Organometallics* **1990**, *9*, 1206−1210.
(53) Harman, W. D.; Wishart, J. F.; Taube, H. *Inorg. Chem.* **1989**, *28*, 2411−2413.
(54) Bart, S. C.; Hawrelak, E. J.; Lobkovsky, E.; Chirik, P. J. *Organometallics* **2005**, *24*, 5518−5527.
(55) Igarashi, R. Y.; Laryukhin, M.; Dos Santos, P. C.; Lee, H.-I.; Dean, D. R.; Seefeldt, L. C.; Hoffman, B. M. *J. Am. Chem. Soc.* **2005**, *127*, 6231−6241.
(56) Barney, B. M.; Laryukhin, M.; Igarashi, R. Y.; Lee, H.-I.; Dos Santos, P. C.; Yang, T.-C.; Hoffman, B. M.; Dean, D. R.; Seefeldt, L. C. *Biochemistry* **2005**, *44*, 8030−8037.
(57) (a) Seefeldt, L. C.; Dance, I. G.; Dean, D. R. *Biochemistry* **2004**, *43*, 1401−1409. (b) Dos Santos, P. C.; Igarashi, R. Y.; Lee, H.-I.; Hoffman, B. M.; Seefeldt, L. C.; Dean, D. R. *Acc. Chem. Res.* **2005**, *38*, 208−214.
(58) Igarashi, R. Y.; Dos Santos, P. C.; Niehaus, W. G.; Dance, I. G.; Dean, D. R.; Seefeldt, L. C. *J. Biol. Chem.* **2004**, *279*, 34770−34775.
(59) Lee, H.-I.; Igarashi, R. Y.; Laryukhin, M.; Doan, P. E.; Dos Santos, P. C.; Dean, D. R.; Seefeldt, L. C.; Hoffman, B. M. *J. Am. Chem. Soc.* **2004**, *126*, 9563−9569.
(60) Lowe, D. J.; Fisher, K.; Thorneley, R. N. F. *Biochem. J.* **1990**, *272*, 621−625.

Table 8. X-ray Diffraction Parameters

	$L^{Me}Fe(HCCPh)$ (**1**)	$L^{Me}Fe(EtCCEt)$ (**2**)	$L^{Me}Fe(CH_2CHPh)$ (**3**)	$L^{Me}Fe(EtCHCHEt)$ (**4**)
empirical formula	$C_{37}H_{47}N_2Fe$	$C_{35}H_{51}N_2Fe$	$C_{37}H_{49}N_2Fe$	$C_{35}H_{53}N_2Fe$
fw	575.628	555.63	577.643	557.654
crystal system	monoclinic	monoclinic	monoclinic	monoclinic
space group	*C*2/*c*	$P2_1/n$	$P2_1/n$	*C*2/*c*
a (Å)	41.313(5)	17.120(2)	13.3997(4)	34.8961(10)
b (Å)	10.2832(12)	17.110(2)	20.5608(7)	11.0547(3)
c (Å)	17.732(2)	23.544(3)	13.7746(5)	20.7338(6)
β (deg)	107.267(2)	103.720(2)	110.3560(10)	122.58
V (Å^3)	7193.6	6699.6(15)	3558.0(2)	6739.9(3)
Z	8	8	4	8
ρ (g cm^{-3})	1.152	1.102	1.078	1.099
μ (mm^{-1})	0.448	0.473	0.488	0.471
R1, wR2 [$I > \sigma(I)$]	0.0426, 0.1088	0.0574, 0.1253	0.0763, 0.2023	0.0458, 0.1285
GOF	1.040	1.077	1.131	1.044

our complexes are not strictly comparable to the enzyme, they can be used to formulate a hypothesis: alkynes may form a stronger enzyme−substrate complex, leading to more efficient reduction.[62] After two-electron reduction, the alkene product would interact with Fe weakly and will be released rather than undergoing further reduction.

Conclusion

In this work, we present a general synthetic method for low-coordinate Fe complexes of the type $L^{Me}Fe$(ligand) with various Lewis bases as the second binding ligand. We also give the first thermodynamic measurements on low-coordinate Fe^I complexes. The ligand binding affinity follows the trend alkynes > alkenes > PPh_3 ∼ benzene > N_2. Electron-withdrawing groups increase the binding affinity, consistent with back-bonding as the dominant contributor to the metal−ligand interaction. Therefore, the formal description of the complexes as Fe^I does not accurately describe the substantial charge transfer to alkyne−alkene ligands. That alkynes are better ligands than alkenes for the low-coordinate Fe center may explain why nitrogenase can reduce alkynes efficiently, but not alkenes.

Experimental Section

General Methods. All manipulations were performed under a N_2 atmosphere using standard Schlenk techniques or in a Braun glovebox maintained at or below 1 ppm of O_2 and H_2O. Glassware was dried at 150 °C overnight. ^{1}H NMR spectra were recorded on a Bruker Avance 400 spectrometer (400 MHz) at 22 °C and referenced internally to a residual protiated solvent (C_6D_5H at 7.15 ppm; $C_6D_{11}H$ at 1.38 ppm). Resonances are broad singlets unless otherwise specified. IR spectra (450−4000 cm^{-1}) were recorded on KBr pellet samples in a Shimadzu FTIR spectrophotometer (FTIR 8400S). A total of 64 scans at a 2-cm^{-1} resolution were collected in each case. Electronic spectra were recorded between 280 and 1100 nm on a Cary 50 UV−vis spectrophotometer, using screw-cap quartz cuvettes of 1-cm optical path length. Elemental analyses were determined by Desert Analytics (Tucson, AZ). Carbon analyses on spectroscopically pure material were often low, possibly from the formation of iron carbide. Pentane, diethyl ether, tetrahydrofuran (THF), and toluene were purified by passage through activated alumina and "deoxygenizer" columns obtained from Glass Contour Co. (Laguna Beach, CA). Deuterated benzene was dried over CaH_2 and then over sodium benzophenone and then vacuum transferred into a storage container. Before use, an aliquot of each solvent was tested with a drop of sodium benzophenone ketyl in a THF solution. Celite was dried overnight at 200 °C under vacuum. Phenylacetylene, *trans*-3-hexene, and styrene were distilled under vacuum prior to use. 3-Hexyne was distilled under vacuum and passed through several short alumina columns until the yellow color on the column disappeared. 4-Ethynylanisole (97%) and 4-ethynyl-α,α,α-trifluorotoluene (97%) were purchased from Aldrich and used as received. The preparation and properties of $[L^{Me}FeCl]_2$ and $L^{Me}FeNNFeL^{Me}$ were previously reported.[8,9]

X-ray Crystallography. Single crystals were mounted on a fiber under Paratone 8277 and immediately placed in a cold N_2 stream at −80 °C on the X-ray diffractometer. The X-ray intensity data were collected on a standard Siemens SMART CCD area detector system equipped with a normal-focus Mo-target X-ray tube operated at 2.0 kW (50 kV, 40 mA). A total of 1321 frames of data (1.3 hemispheres) were collected using a narrow-frame method with scan widths of 0.3° in ω and exposure times varying from 10 to 60 s frame^{-1} using a detector-to-crystal distance of 5.09 cm (maximum 2θ angle of 56.5°). The total data collection time was typically between 12 and 24 h. Frames were integrated to a maximum 2θ angle of 56.5° with the Siemens SAINT program. Laue symmetry revealed the crystal systems, and the final unit cell parameters (at −80 °C) were determined from the least-squares refinement of the three-dimensional centroids of the reflections. Data were corrected for absorption with *SADABS*. The space groups were assigned using XPREP, and the structures were solved with direct methods by using Sir92 (WinGX, version 1.63.02) and refined by employing full-matrix least squares on F^2 (*SHELXTL*, version 5.04). The X-ray diffraction data collection parameters are shown in Table 8. All of the atoms were refined with anisotropic thermal parameters unless otherwise noted. H atoms were included in idealized positions unless otherwise specified.

The structure of **1** contained a disordered solvent molecule, which was removed from the data (135 e$^-$ in 843.1 Å^3 per unit cell) using the SQUEEZE function of *PLATON*. The structure of **4** contained a disordered $CH_3CH_2CH{=}CHCH_2CH_3$ group. C34 and C44 of the hexene are disordered in a 1:2 ratio for parts A and B, respectively. The rest of the hexene was modeled in a single part.

(61) A reviewer has correctly noted a weakness of this model: the order of the binding affinities here, alkene > N_2, is inconsistent with the fact that N_2 is reduced by the enzyme but alkenes are not. However, we note that the geometries for alkyne or alkene binding versus N_2 binding are often different, and that alkyne binding and N_2 binding are thought to occur in different oxidation levels of iron−molybdenum nitrogenase. Clearly, the hypothesis advanced here should be tested using other model complexes and the enzyme itself.

(62) Consistent with the relative binding constants described here, the apparent dissociation constant for acetylene on the FeMoco (as derived from EPR studies on *K. pneumoniae* nitrogenase) is much lower than that for ethylene: Lowe, D. J.; Eady, R. R.; Thorneley, R. N. F. *Biochem. J.* **1978**, *173*, 277−290.

$L^{Me}Fe(HC{\equiv}CPh)$ (1). A Schlenk flask was loaded with a solution of $L^{Me}FeNNFeL^{Me}$ (100 mg, 103 μmol) in pentane (10 mL). Phenylacetylene (23 μL, 206 μmol) was added via syringe to the dark-red solution, causing immediate effervescence. The solution was stirred at room temperature for 30 min and concentrated to 3 mL. Crystallization from pentane at −35 °C gave dark-red needles (88 mg, 74%). ^{1}H NMR (400 MHz, C_6D_6): 74 (1H, backbone C−H), 35 (6H, backbone CH_3), 14 (1H, PhCCH, *p*-H), 13 (2H, PhCCH, *m*-H), −12 (12H, ^{i}Pr methyl), −13 (4H, *m*-H), −25 (2H, *p*-H), −69 (12H, ^{i}Pr methyl), −83 (4H, ^{i}Pr methine) ppm. IR (KBr pellet): 1717 cm^{-1} (C≡C). UV−vis (toluene): 328 (ϵ = 15.7 mM^{-1} cm^{-1}), 395 (ϵ = 6.8 mM^{-1} cm^{-1}), 524 (ϵ = 0.6 mM^{-1} cm^{-1}), 738 (ϵ = 0.2 mM^{-1} cm^{-1}) nm. μ_{eff} (C_6D_6, 25 °C): 4.7(7) μ_B. Elem anal. Calcd for $C_{37}H_{47}N_2Fe$: C, 77.20; H, 8.23; N, 4.87. Found: C, 76.87; H, 8.10; N, 4.86. The other Fe complexes were synthesized through an analogous route.

$L^{Me}Fe(EtC{\equiv}CEt)$ (2). Synthesized similarly to **1** using 3-hexyne. Yield 79%. ^{1}H NMR (400 MHz, C_6D_6): 124 (4H, CH_3CH_2-C≡CCH_2CH_3), 91 (1H, backbone C−H), 48 (6H, $CH_3CH_2C{\equiv}CCH_2CH_3$), 37 (6H, backbone CH_3), −14 (12H, ^{i}Pr methyl), −18 (4H, *m*-H), −25 (2H, *p*-H), −77 (12H, ^{i}Pr methyl), −86 (4H, ^{i}Pr methine) ppm. IR (KBr pellet): 1802 cm^{-1} (C≡C). UV−vis (toluene): 329 (ϵ = 12.3 mM^{-1} cm^{-1}), 395 (ϵ = 7.2 mM^{-1} cm^{-1}), 512 (ϵ = 0.6 mM^{-1} cm^{-1}) nm. μ_{eff} (C_6D_6, 21 °C): 4.4(8) μ_B. Elem anal. Calcd for $C_{35}H_{51}N_2Fe$: C, 75.66; H, 9.25; N, 5.04. Found: C, 73.86; H, 9.18; N, 5.27.

$L^{Me}Fe(CH_2{=}CHPh)$ (3). Synthesized similarly to **1**, using styrene. Yield 72%. ^{1}H NMR (400 MHz, toluene-d_8): 78 (2H), 62 (1H, styrene *p*-H), 40 (6H, backbone CH_3), 19 (1H, backbone H), 11 (2H), 5 (2H), 0 (6H, ^{i}Pr methyl), −5 (6H, ^{i}Pr methyl), −14 (2H), −18 (2H), −29 (6H, ^{i}Pr methyl), −34 (6H, ^{i}Pr methyl), −77 (2H) ppm. There are six signals that integrate to two protons [L(Ar)−*o*-H, L(Ar)−*m*-H, L(Ar)−*p*-H, styrene−*o*-H, styrene−*m*-H, and ^{i}Pr methine], which were not assigned specifically. UV−vis (toluene): 319 (ϵ = 18.8 mM^{-1} cm^{-1}), 374 (ϵ = 11.7 mM^{-1} cm^{-1}) nm. μ_{eff} (C_6D_6, 25 °C): 4.8(7) μ_B. Elem anal. Calcd for $C_{37}H_{49}N_2Fe$: C, 76.93; H, 8.55; N, 4.85. Found: C, 70.45; H, 8.54; N, 4.84.

$L^{Me}Fe(EtCH{=}CHEt)$ (4). Synthesized similarly to **1**, using *trans*-3-hexene. Yield 52%. ^{1}H NMR (400 MHz, cyclohexane-d_{12}): 29 (1H, backbone H), 14 (6H, backbone CH_3), 7.6(3H, EtCH=CHCH$_2$CH_3), 7.0 (3H, CH_3CH$_2$CH=CHEt), 6.0 (2H), −1 (6H, ^{i}Pr methyl), −2 (6H, ^{i}Pr methyl), −21 (2H), −30 (6H, ^{i}Pr methyl), −38 (6H, ^{i}Pr methyl), −47 (2H), −54 (2H), −56 (2H), −103 (2H). There are six signals that integrate to two protons [L(Ar)−*o*-H, L(Ar)−*m*-H, L(Ar)−*p*-H, styrene−*o*-H, styrene−*m*-H, and ^{i}Pr methine), which were not assigned specifically. UV−vis (pentane): 315 (ϵ = 18.4 mM^{-1} cm^{-1}), 367 (ϵ = 10.4 mM^{-1} cm^{-1}), 471 (1.9 mM^{-1} cm^{-1}) nm. μ_{eff} (C_6D_6, 25 °C): 4.3(7) μ_B. Elem anal. Calcd for $C_{35}H_{53}N_2Fe$: C, 75.38; H, 9.58; N, 5.02. Found, C, 69.71; H, 8.90; N, 5.42.

$L^{Me}Fe$(4-ethynylanisole) (5). Sunthesized similarly to **1**, using 4-ethynylanisole. Yield 90%. ^{1}H NMR (400 MHz, C_6D_6): 76 (1H, backbone C−H), 34 (6H, backbone CH_3), 12 (2H, HC≡CC_6H_4-OCH_3 *o*/*m*-H), 11 (3H, HC≡C$C_6H_4OCH_3$), 10 (1H, *H*C≡CC_6H_4-OCH_3), −12 (12H, ^{i}Pr methyl), −13 (4H, *m*-H), −25 (2H, *p*-H), −71 (12H, ^{i}Pr methyl), −85 (4H, ^{i}Pr methine) ppm. IR (KBr pellet): 1717 cm^{-1} (C≡C). UV−vis (toluene): 328 (ϵ = 15.4 mM^{-1} cm^{-1}), 395 (ϵ = 6.2 mM^{-1} cm^{-1}), 520 (ϵ = 0.6 mM^{-1} cm^{-1}), 715 (ϵ = 0.2 mM^{-1} cm^{-1}) nm.

$L^{Me}Fe$(4-ethynyl-α,α,α-trifluorotoluene) (6). Synthesized similarly to **1**, using 4-ethynyl-α,α,α-trifluorotoluene. Yield 88%. ^{1}H NMR (400 MHz, C_6D_6): 72 (1H, backbone C−H), 34 (6H, backbone CH_3), 14 (2H, HC≡C$C_6H_4CF_3$ *o*/*m*-H), 10 (1H, *H*C≡C$C_6H_4CF_3$), −12 (12H, ^{i}Pr methyl), −13 (4H, *m*-H), −26 (2H, *p*-H), −69 (12H, ^{i}Pr methyl), −82 (4H, ^{i}Pr methine) ppm. IR (KBr pellet): 1720 cm^{-1} (C≡C). UV−vis (toluene): 328 (ϵ = 14.7 mM^{-1} cm^{-1}), 395 (ϵ = 5.9 mM^{-1} cm^{-1}), 527 (ϵ = 0.6 mM^{-1} cm^{-1}), 734 (ϵ = 0.2 mM^{-1} cm^{-1}) nm.

Equilibrium Constants. An excess of free ligands A and B was added to a solution of $L^{Me}Fe$(ligand A) (0.08−0.5 mM). The concentrations of Fe complexes were calculated as

$$a_1[L^{Me}Fe(\text{ligand A})] + b_1[L^{Me}Fe(\text{ligand B})] + c_1 = A_1$$

$$a_2[L^{Me}Fe(\text{ligand A})] + b_2[L^{Me}Fe(\text{ligand B})] + c_2 = A_2$$

A_1 and A_2 are UV−vis absorptions at λ_{max} for $L^{Me}Fe$(ligand A) and $L^{Me}Fe$(ligand B), respectively; a_1, a_2, b_1, and b_2 are extinction coefficients for complexes $L^{Me}Fe$(ligand A) and $L^{Me}Fe$(ligand B) at wavelengths 1 and 2; c_1 and c_2 are background absorptions obtained by taking the UV−vis spectrum of a pure solvent with a free ligand. The derived concentrations were used to calculate equilibrium constants according to eq 1. All of the error bars are calculated from the extinction coefficient. Details on the absorption maxima, free ligand concentrations, calculated Fe complex concentrations, and equilibrium constants are given in the Supporting Information.

Acknowledgment. This work was funded by the National Science Foundation (Grant CHE-0112658) and the National Institutes of Health (Grant GM065313-02). P.L.H. is a Alfred P. Sloan Fellow.

Note Added after ASAP Publication. This article was released ASAP on April 21, 2006, with incorrect compound numbers in the phrase "Synthesized similarly to ...". The correct version was posted on April 24, 2006. A further corrected version with a change to ref 62 was posted on June 26, 2006.

Supporting Information Available: Details on equilibrium measurements (PDF) and crystallography (CIF). This material is available free of charge via the Internet at http://pubs.acs.org.

IC052136+